

1           **Development of high spatial resolution annual**  
2           **emission inventory of greenhouse gases from open**  
3           **straw burning in Northeast China from 2001 to 2020**

4           Zihan Song<sup>a,b</sup>, Leiming Zhang<sup>c</sup>, Chongguo Tian<sup>d</sup>, Qiang Fu<sup>a,b</sup>, Zhenxing Shen<sup>e</sup>,  
5   Renjian Zhang<sup>f</sup>, Dong Liu<sup>a,b</sup>, Song Cui<sup>a,b\*</sup>

6           <sup>a</sup> *International Joint Research Center for Persistent Toxic Substances (IJRC-PTS), School of*  
7           *Water Conservancy and Civil Engineering, Northeast Agricultural University, Harbin,*  
8           *Heilongjiang, 150030, China*

9           <sup>b</sup> *Research Center for Eco-Environment Protection of Songhua River Basin, Northeast*  
10           *Agricultural University, Harbin, Heilongjiang, 150030, China*

11           <sup>c</sup> *Air Quality Research Division, Science and Technology Branch, Environment and Climate*  
12           *Change Canada, Toronto, Ontario, M3H 5T4, Canada*

13           <sup>d</sup> *CAS Key Laboratory of Coastal Environmental Processes and Ecological Remediation,*  
14           *Yantai Institute of Coastal Zone Research, Chinese Academy of Sciences, Shandong Key*  
15           *Laboratory of Coastal Environmental Processes, YICCAS, Yantai, 264003, China*

16           <sup>e</sup> *Department of Environmental Sciences and Engineering, Xi'an Jiaotong University, Xi'an,*  
17           *710049, China*

18           <sup>f</sup> *Institute of Atmospheric Physics, Chinese Academy of Sciences, Beijing 100029, China*

19           \*Corresponding author: Dr. Song Cui           Email: cuisong-bq@neau.edu.cn (S. Cui)

20  
21  
22  
23           **WORD COUNT: 6000**

24           **7 FIGURES**

25           **1 TABLE**

26 **Abstract**

27 Open straw burning has been widely recognized as a significant source of greenhouse  
28 gases (GHGs), posing critical risks to atmospheric integrity and potentially  
29 exacerbating global warming. In this study, we proposed a novel method that integrates  
30 crop cycle information into extraction and classification of fire spots from open straw  
31 burning in Northeast China from 2001 to 2020. By synergizing the extracted fire spots  
32 with the modified Fire Radiative Power (FRP) algorithm, we developed high spatial  
33 resolution emission inventories of GHGs, including carbon dioxide (CO<sub>2</sub>), methane  
34 (CH<sub>4</sub>), and nitrous oxide (N<sub>2</sub>O). Results showed that the northern Sanjiang Plain,  
35 eastern Songnen Plain, and eastern Liao River Plain were areas with high intensity of  
36 open straw burning. The number of fire spots was **evaluated** during 2013-2017,  
37 accounting for **58.2%** of the total fire spots observed during 2001-2020. The prevalent  
38 season for open straw burning shifted from autumn (pre-2016) to spring (post-2016),  
39 accompanied by a more dispersed pattern in burning dates. The two-decade cumulative  
40 emissions of CO<sub>2</sub>, CH<sub>4</sub>, and N<sub>2</sub>O were quantified at **198 Tg**, **557 Gg**, and **15.7 Gg**,  
41 respectively, amounting to **218 Tg** of CO<sub>2</sub>-eq. Significant correlations were identified  
42 between GHGs emissions and both straw yields and straw utilization ( $p < 0.01$ ). The  
43 enforcement of straw burning bans since 2018 has played a pivotal role in curbing open  
44 straw burning, and reduced fire spots by **51.7%** on annual basis compared to 2013-2017.  
45 The novel method proposed in this study considerably enhanced the accuracy in  
46 characterizing spatiotemporal distributions of fire spots from open straw burning and

47 quantifying associated pollutants emissions.

48 **Keywords:** Open straw burning; Fire spot; Crop cycle; Greenhouse gas; Emission

49 inventory

50 **Keywords Plus:** Open straw burning; MODIS; Fire spot; Accurate extraction; Crop

51 cycle; Crop type; Phenology; Greenhouse gas; Emission inventory; Driving factor;

52 Policy

53 **Copyright statement.** The works published in this journal are distributed under the

54 Creative Commons Attribution 4.0 License. This license does not affect the Crown

55 copyright work, which is re-usable under the Open Government Licence (OGL). The

56 Creative Commons Attribution 4.0 License and the OGL are interoperable and do not

57 conflict with, reduce or limit each other.

58 © Crown copyright 2024.

59

## 60 1 Introduction

61 Open straw burning, a customary practice in agricultural areas, serves multiple purposes,  
62 including rapid straw disposal, weed control, nutrient release, and pest management  
63 (Korontzi et al., 2006; Wen et al., 2020). This practice results in short-term yet intense  
64 emissions of greenhouse gases (GHGs), such as carbon dioxide (CO<sub>2</sub>), methane (CH<sub>4</sub>),  
65 and nitrous oxide (N<sub>2</sub>O). The accumulation of these gases in the atmosphere adversely  
66 impacts climate and atmospheric chemistry (Weldemichael and Assefa, 2016; Tang et  
67 al., 2020; Hong et al., 2023). To date, open straw burning **remains prevalent** in grain-  
68 producing areas globally, despite the many drawbacks of such a practice (Gadde et al.,  
69 2009; Huang et al., 2013; Zhu et al., 2015; Ahmed et al., 2019; Mehmood et al., 2020;  
70 Fu et al., 2022; Huang et al., 2023; Xu et al., 2023a). Thus, accurate and high spatial  
71 resolution emission inventories for GHGs from this source sector are needed from  
72 regional to global scales to assess potential climate and air quality impacts and  
73 formulate carbon mitigation policies.

74

75 The “bottom-up” approach, which is based on the amount of straw burned and  
76 corresponding emission factors, has been widely employed to establish emission  
77 inventories for various pollutants emitted from open straw burning (van der Werf et al.,  
78 2017; Wang et al., 2018; Liu et al., 2021; Zheng et al., 2023). Emission factors for  
79 diverse pollutants released from different types of straw burning have been extensively  
80 investigated in laboratory studies (Li et al., 2007; Liu et al., 2011; Stockwell et al., 2014;

81 Pan et al., 2017; Peng et al., 2016; Sun et al., 2016). However, estimation of the amount  
82 of straw burned is subject to large uncertainties since it involves many parameters, such  
83 as grain yield, ratio of straw and grain, open burning proportion, burning efficiency,  
84 and dry matter fraction (Guan et al., 2017; Zhou et al., 2017). Consequently, existing  
85 regional-scale emission inventories based on the “bottom-up” approach generally have  
86 large uncertainties and low spatiotemporal resolutions (Tian et al., 2011; Jin et al., 2017).  
87  
88 The advent of satellite technologies, such as Moderate Resolution Imaging  
89 Spectroradiometer (MODIS, remote sensing instrument), Visible Infrared Imaging  
90 Radiometer Suite (VIIRS, remote sensing instrument), and Himawari-8 (geostationary  
91 satellite), has markedly revolutionized the monitoring of open straw burning, enabling  
92 real-time and high spatiotemporal resolution fire spot products to be accessible to the  
93 general public (Schroeder et al., 2014; Giglio et al., 2016; Xu et al., 2017; Wu et al.,  
94 2018; Zhuang et al., 2018; Lv et al., 2024). Many studies have effectively utilized  
95 satellite fire spot products for constructing emission inventories, based on either the  
96 burned area (BA) or fire spot counts (FC) (Ke et al., 2019; Cui et al., 2021). **Several**  
97 **studies have also developed a hybrid inventory strategy using the “bottom-up”**  
98 **approach to allocate GHGs emissions spatially and temporally based on BA or FC (Jin**  
99 **et al., 2018; Zhang et al., 2019; Kumar et al., 2021). These approaches have**  
100 **significantly improved the spatiotemporal resolutions of the emission inventories for**  
101 **open straw burning (Wu et al., 2023).**

102

103 MODIS and VIIRS, both operating in polar orbits, provide only two observations per  
104 day. MODIS has provided 1 km resolution fire data since 2000, which is suitable for  
105 long-term trend analyses (Chen et al., 2012); while VIIRS has provided fire data at a  
106 375 m resolution since 2012, which is more suitable for detecting small fires (Chen et  
107 al., 2022). Himawari-8 (Geostationary orbit) has provided 10-minute temporal  
108 resolution and 2 km spatial resolution fire data since 2015, ideal for real-time  
109 monitoring across the Asia-Pacific region (Zhang et al., 2020). However, the  
110 aforementioned datasets remain inadequate for accurately capturing small-area, short-  
111 duration open straw burning, particularly in scattered farmlands (Wiedinmyer et al.,  
112 2014). It should also be noted that meteorological disturbances, such as cloud cover and  
113 rainfall, can reduce the accuracy of these products (Schroeder et al., 2014; Ying et al.,  
114 2019). Furthermore, straw burning during non-satellite transit periods, on cloudy days,  
115 at night, and under heavy haze may not be captured in these datasets (Liu et al., 2020).  
116 For example, Liu et al. (2019) found that same-day omission error of MODIS burned  
117 area product could be as high as 95% for agricultural fire detection during the post-  
118 monsoon season in northwestern India.

119

120 With continuous enrichment of satellite data, a strong relationship was observed  
121 between fire radiative power (FRP) and emission amounts from open straw burning  
122 (Wu et al., 2023). Consequently, the FRP algorithm has been widely accepted for

123 estimating emissions (Wooster et al., 2005; Freeborn et al., 2008; Vermote et al., 2009;  
124 Yang et al., 2019). The FRP algorithm has been optimized by integrating multi-source  
125 satellite fire spot data, field survey data, and ground observation data, and combined  
126 with advanced modeling techniques to improve the accuracy of emission inventory for  
127 open straw burning. For example, Liu et al. (2020) revised FRP by combining  
128 household survey results with satellite observations in northern India to capture small  
129 fires, fill cloud/haze gaps in satellite observations, and adjust partial-field burns and  
130 diurnal cycle of fire activity disturbances. Yang et al. (2020) improved the FRP  
131 algorithm by calibrating the contributions of open straw burning to ground observation  
132 data in Northeast China based on model simulation results using the coupled Weather  
133 Research and Forecasting model and Community Multiscale Air Quality (WRF-CMAQ)  
134 model.

135

136 At present, the identification of straw types in open straw burning typically relies on  
137 crop data, such as the International Geosphere-Biosphere Programme (IGBP)-Modified  
138 MODIS Land Use and MapSPAM datasets (Ke et al. 2019; Yang et al. 2020). These  
139 low spatiotemporal resolution crop data contribute to errors in both the extraction of  
140 fire spots and the identification of straw types (Ke et al., 2019; Liu et al., 2022).  
141 Additional errors come from planting structure adjustment and frequent variations in  
142 crop phenology. For instance, fire spots occurred during crop growth might be  
143 incorrectly classified as open straw burning, while those occurred prior to crop growth

144 could be inaccurately attributed to burning of straws from subsequent harvests (Zhou  
145 et al., 2022). Therefore, high spatiotemporal resolution data on crop types and  
146 phenology are critical, and such data should be integrated into the extraction and  
147 classification of fire spots from open straw burning to accurately estimate emissions of  
148 various pollutants from this source sector.

149

150 To control emissions from open straw burning, the “Air Pollution Prevention and  
151 Control Action Plan” (APPCAP) took into effect in 2013 in China (Huang et al., 2021).  
152 In addition, China committed to achieve carbon peak by 2030 and carbon neutrality by  
153 2060, which draws unprecedented challenges in reducing carbon emissions from open  
154 straw burning (Wu et al., 2023). As a significant grain-producing region in China,  
155 Northeast China produced 135 million tons of major grains (corn, rice, beans, and wheat)  
156 in 2020, accounting for 21.4% of total production in China (National Bureau of  
157 Statistics of China, 2021). During 2013-2018, open straw burning in Northeast China  
158 exhibited an increasing trend, while decreasing in all other regions of China (Huang et  
159 al., 2021). The constant increase reflects the expansion of the agricultural sector and  
160 economic development in Northeast China yet relatively unconstrained open burning  
161 activities (Huang et al., 2021). Liu et al. (2022) estimated CO<sub>2</sub> emissions from open  
162 straw burning in Northeast China to be as high as 344 Tg from 2012 to 2020.

163

164 In this study, high spatial resolution fire spot products were used to develop annual



165 emission inventories of GHGs, including CO<sub>2</sub>, CH<sub>4</sub>, and N<sub>2</sub>O, from open straw burning  
166 in Northeast **China** for the period of 2001-2020. To improve the accuracy of the  
167 developed emission inventory, a novel concept that integrates the crop cycle  
168 information into fire spot extraction and classification was adopted. Furthermore, this  
169 study conducted a thorough analysis to assess the driving factors influencing GHGs  
170 emissions during the two decades. This study comprehensively examined GHGs  
171 emissions from open straw burning in Northeast China and offered valuable insights to  
172 policy makers for mitigating carbon emissions and air pollution in agricultural areas.

## 173 **2 Methodology**

### 174 **2.1 Extraction and classification of fire spots**

175 **The MODIS fire product (MCD14ML, Collection 6.1) was selected from 1 January**  
176 **2001 to 31 December 2020 for the whole region of Northeast China (Giglio et al., 2016,**  
177 **[sftp://fuoco.geog.umd.edu](http://fuoco.geog.umd.edu)). The dataset, with a spatial resolution of about 1 km<sup>2</sup>,**  
178 **includes essential variables, such as latitude, longitude, acquisition date and time (in**  
179 **UTC), satellite (Aqua or Terra), FRP, and fire type (presumably vegetation fire, active**  
180 **volcano, other static land source, and offshore), among others ([https://modis-](https://modis-fire.umd.edu/files/MODIS_C6_C6.1_Fire_User_Guide_1.0.pdf)**  
181 **[fire.umd.edu/files/MODIS\\_C6\\_C6.1\\_Fire\\_User\\_Guide\\_1.0.pdf](https://modis-fire.umd.edu/files/MODIS_C6_C6.1_Fire_User_Guide_1.0.pdf)). Non-vegetation fire**  
182 **activities (active volcano, other static land source, and offshore) were then filtered out**  
183 **from the selected dataset for subsequent analysis.**

184

185 To clarify, the MCD14ML underestimated fire spots in 2001 and 2002 because only the  
186 Terra satellite was operational before 3 July 2002. Therefore, data for the years of 2003  
187 to 2020 were used for developing annual emission inventories, with relevant results for  
188 2001 and 2002 as reference only. Also, a failure of the Aqua satellite on 16 August 2020  
189 led to the loss of fire spot data for about two weeks ([https://modis-  
190 fire.umd.edu/files/MODIS\\_C61\\_BA\\_User\\_Guide\\_1.1.pdf](https://modis-fire.umd.edu/files/MODIS_C61_BA_User_Guide_1.1.pdf)). However, as August is a  
191 crop-growing period in Northeast China, this failure would not lead to an  
192 underestimation of fire spots from open straw burning.

193

194 The ChinaCropArea1 km and ChinaCropPhen1 km datasets were used to extract and  
195 classify fire spots from open straw burning (Luo et al., 2020a; Luo et al., 2020b). These  
196 datasets present annual data on the type and phenology (Day of Year (Doy) of  
197 emergence and maturity) of grain crops (corn, rice, and wheat). Considering that  
198 Northeast China is a major bean-producing area, we also compiled bean distribution  
199 datasets (Li et al., 2021; Xuan et al., 2023). However, bean distribution in Jilin and  
200 Liaoning provinces was not recorded during 2001-2012 in this dataset. The dataset was  
201 extended to the whole region of Northeast China (Heilongjiang, Jilin, and Liaoning  
202 provinces) after 2013. Thus, some gaps still exist in these datasets compared to the  
203 comprehensive information required for this study, as detailed in **Table S1**.

204

205 **Fig. 1** describes the meticulous process to accurately extract and classify fire spots from

206 open straw burning in areas experiencing one-harvest season every year. The process  
207 involves several key steps:

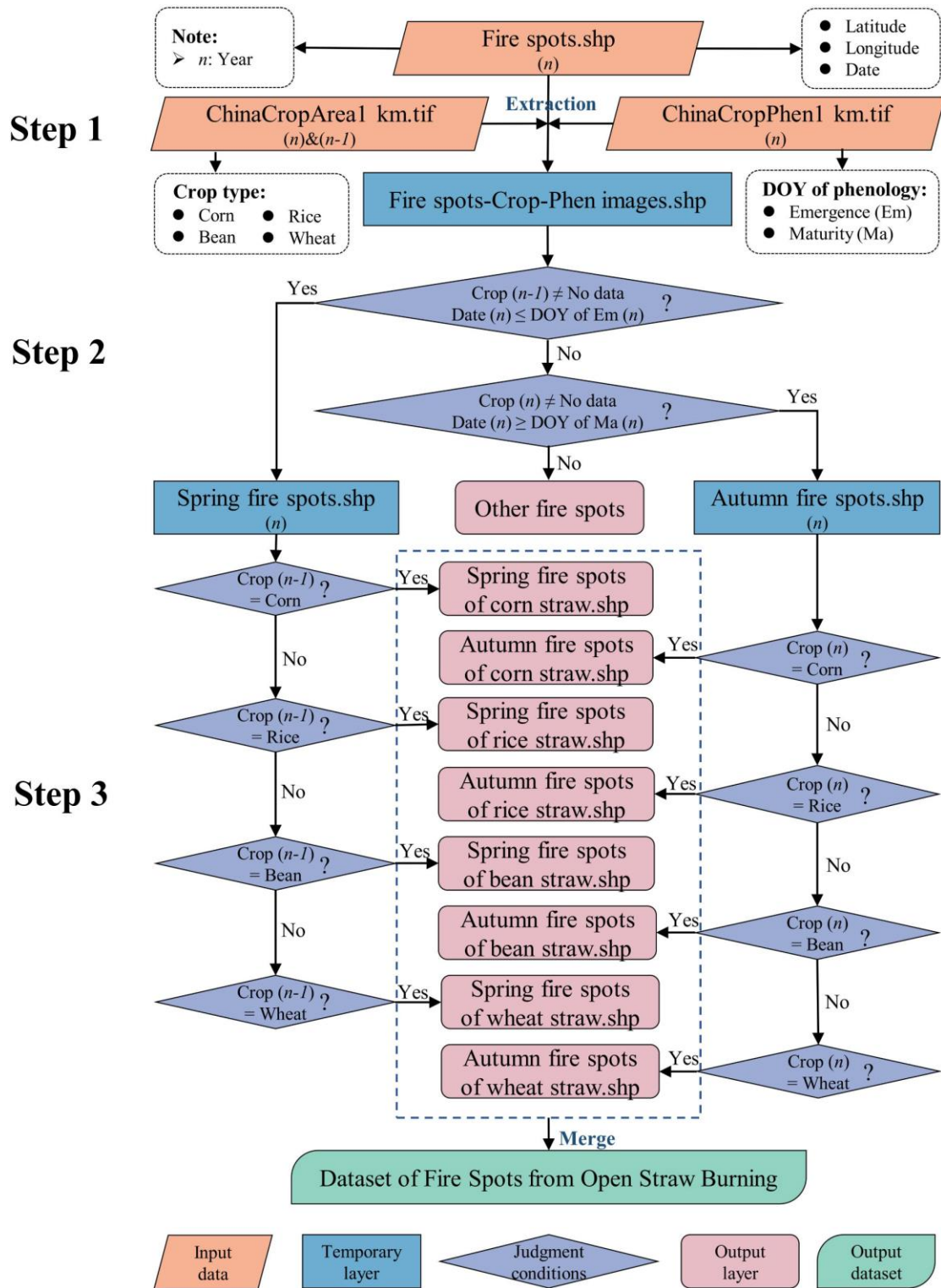
208 **Step 1)** The current year's ChinaCropPhen1 km and ChinaCropArea1 km, along with  
209 the previous year's ChinaCropArea1 km data, were extracted to Fire spots (MCD14ML)  
210 by ArcGIS 10.2 software to obtain the Fire spots-Crop-Phen dataset.

211 **Step 2)** Considering the crop cycle, the extraction of fire spots was divided into two  
212 stages. The first stage is before crop growth (spring) and requires the fire spot to satisfy  
213 two conditions: a) there was a crop planted in the previous year, and b) the burning date  
214 is before emergence. The second stage is after crop growth (autumn) and also involves  
215 two conditions: a) there was a crop planted in the current year, and b) the burning date  
216 is after maturity.

217 **Step 3)** For fire spots in spring, the type of straw burned is identified based on the  
218 previous year's crop type. For autumn fire spots, the straw type is determined according  
219 to the crop type of the current year.

220

221 **Furthermore, fire spots from open straw burning were extracted using the traditional**  
222 **method that does not integrate crop cycle information. Only the current year's**  
223 **ChinaCropArea1 km data was extracted to Fire spots (MCD14ML). Then, fire spots**  
224 **occurring on agricultural land with growing crops were identified as open straw burning.**



225

226 **Fig. 1** Extraction and classification method for fire spots from open straw burning

227 **2.2 Development of high spatial resolution annual emission inventories for**  
228 **GHGs and exploration of driving factors**

229 Annual emission inventories for GHGs were developed for the region of Northeast  
230 China at a grid resolution of 5 km × 5 km for the years of 2001 to 2020. The domain  
231 grids were created using Fishnet of ArcGIS 10.2 software.

232

233 The modified FRP algorithm (Yang et al., 2020) is used to estimate the emissions of  
234 GHGs from open straw burning in this study:

235 
$$E = \alpha \times \int_{t_1}^{t_2} FRP^* dt \times \beta \times F = \alpha \times FRP \times f_{FRP} \times (t_2 - t_1) \times \beta \times F \quad (1)$$

236 where  $E$  (in g) is the emissions of GHGs;  $\alpha$  is a correction factor used to adjust for  $FRP$   
237 detection errors between MODIS and VIIRS, which is given a value of 2.5 following  
238 Vadrevu and Lasko (2018), indicating that the  $FRP$  VIIRS sum is 2.5 times of the  $FRP$   
239 MODIS sum;  $t_1$  and  $t_2$  are the beginning and ending time of fire spots, respectively, and  
240 the average burning time (3 hours) of a fire spot in Northeast China was obtained by  
241 delivering questionnaires to local farmers (Yang et al., 2020);  $FRP^*$  (in MW) is adjusted  
242 satellite detected  $FRP$ ;  $FRP$  (in MW) is the instantaneous  $FRP$  observed by satellite;  
243  $f_{FRP}$  is a correction factor that is used to adjust the underestimated emissions by fire  
244 spots, and Yang et al. (2020) determined an optimal value of 5 for  $f_{FRP}$  by calibrating  
245 the contributions of open straw burning to ground observation data in Northeast China  
246 using WRF-CMAQ;  $\beta$  (in kg·MJ<sup>-1</sup>) is biomass combustion rate and the average value  
247 of 0.411 kg·MJ<sup>-1</sup> from previous studies is used here (Wooster et al., 2005; Freeborn et

248 al., 2008); and  $F$  (in  $\text{g}\cdot\text{kg}^{-1}$ ) is the emission factor for individual straw type (**Table 1**)  
249 (Li et al., 2007; Liu et al., 2011; Peng et al., 2016).

250

251 **Table 1.** Emission factors of open straw burning for different crop types

Crop	Emission factors ( $\text{g}\cdot\text{kg}^{-1}$ )		
	CO <sub>2</sub>	CH <sub>4</sub>	N <sub>2</sub> O
Corn	1350	4.4	0.12
Rice	1460	3.2	0.11
Bean	1445	3.9	0.09
Wheat	1460	3.4	0.05

252

253 Driving factors such as the output of major grains and rural residential coal  
254 consumption for temporal variations of annual GHGs emissions were explored through  
255 Pearson correlation analysis using SPSS 20.0. Information on the above data is also  
256 detailed in **Table S1**.

### 257 **3 Results and discussion**

#### 258 **3.1 Spatial and temporal distributions of fire spots**

259 Cultivated lands in Northeast China primarily distribute in Sanjiang Plain (Northeast  
260 Heilongjiang Province), Songnen Plain (West Heilongjiang Province and Midwest Jilin  
261 Province), and Liao River Plain (Central Liaoning Province) (**Fig. 2(a)**). Fire spots were  
262 widely spread, covering most cultivated lands, including both dry and paddy fields  
263 across Northeast China (**Fig. 2(a)** and **2(b)**). A total of 156,044 fire spots from open  
264 straw burning were recorded during 2001-2020. Note that the traditional method

265 overestimated the total number of fire spots by 7190 over the 20-year period, with the  
266 largest error in 2017 (an overestimation of 4060) (**Fig. 2(c)**). This highlights the  
267 importance of integrating crop cycle information into fire spot extraction for open straw  
268 burning to enhance data accuracy and reliability. Considering the 20-year together  
269 (2001-2020), high occurrence frequencies of open straw burning (also referred to as  
270 intensity of fire spots below) appeared in the northern Sanjiang Plain, eastern Songnen  
271 Plain, and eastern Liao River Plain, as well as scattered areas close to Inner Mongolia  
272 (**Fig. 2(a)** and **2(b)**).

273

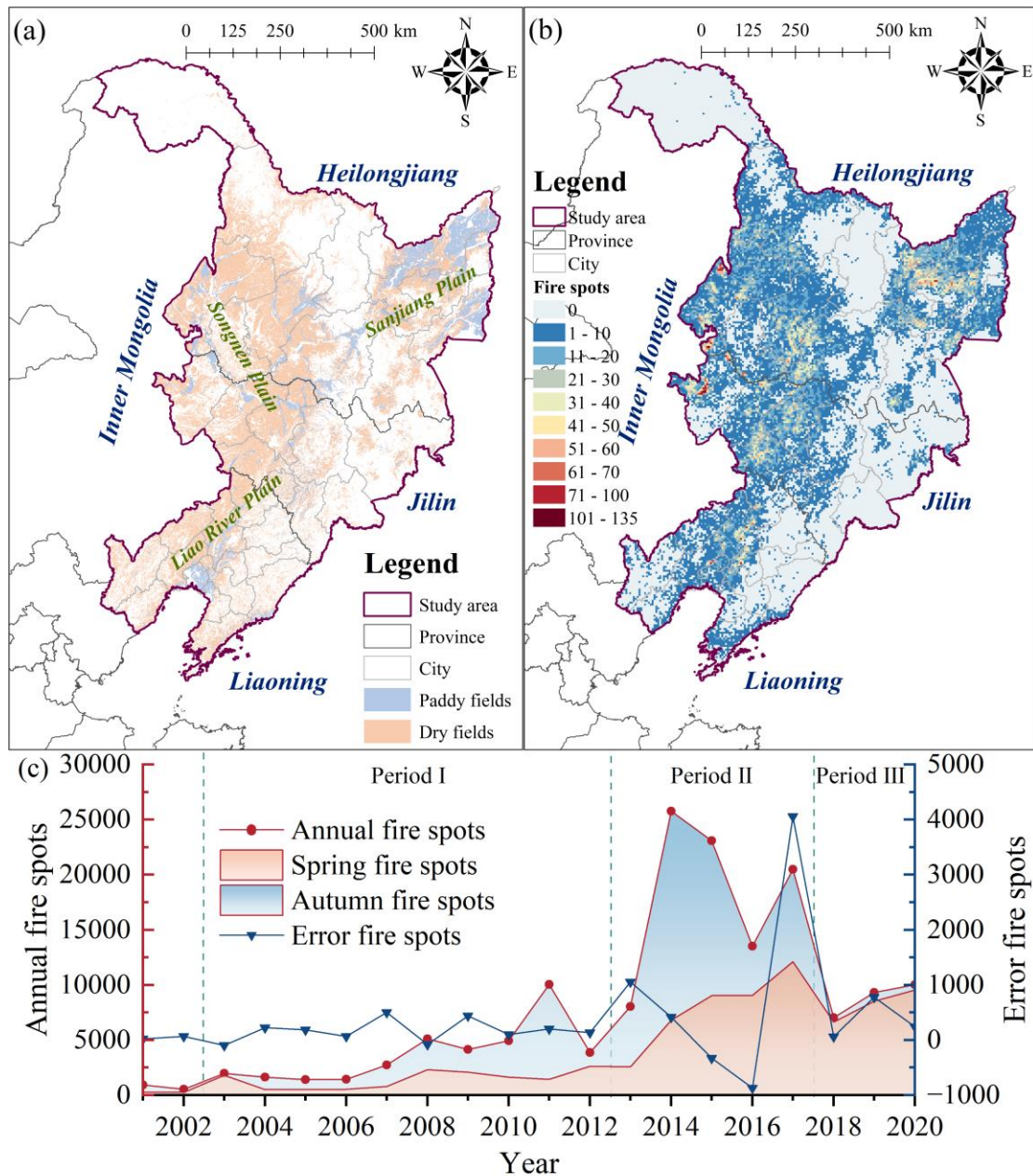
274 Interannual variations of fire spots distributions are shown in **Fig. S1**. In the Sanjiang  
275 Plain, low occurrence frequencies of fire spots were observed in a few cultivated lands  
276 during 2003-2006 (**Fig. S1(c)** to **Fig. S1(f)**) and in most cultivated lands in the northern  
277 part of the Plain during 2007-2013 (**Fig. S1(g)** to **Fig. S1(m)**). Note that in 2014 and  
278 later years, fire spots were extended to the entire Sanjiang Plain, and the northern part  
279 of the Plain became an area with high intensity of fire spots (**Fig. S1(n)** to **Fig. S1(q)**),  
280 although a few cultivated lands in this Plain recorded low intensity of fire spots after  
281 2018 (**Fig. S1(r)** to **Fig. S1(t)**). In the Songnen Plain, most cultivated lands recorded  
282 fire spots during 2014 to 2017, with highest intensity in the northern and eastern parts  
283 of the Plain (**Fig. S1(n)** to **Fig. S1(q)**). The occurrence frequencies of fire spots  
284 decreased across the plain since 2018, particularly in the northern part of the Plain (**Fig.**  
285 **S1(r)** to **Fig. S1(t)**). In the Liao River Plain, although fire spots were observed in most

286 cultivated lands in the eastern part of the Plain during 2014-2017, high occurrence  
287 frequency was only recorded in 2014 (**Fig. S1(n)** to **Fig. S1(q)**).

288

289 Apparently, open straw burning events decreased in all of the three Plains since 2018  
290 (**Fig. S1(r)** to **Fig. S1(t)**), which was likely due to the intensified effort from the Chinese  
291 government banning open straw burning (Hong et al., 2023). The reduction in the  
292 number of fire spots was more significant in the Sanjiang Plain and northern Songnen  
293 Plain than Liao River Plain (**Fig. S1**), indicating more compliance with straw burning  
294 bans from State Farms in the former two regions.





295

296 **Fig. 2** (a) Spatial distributions of cultivated land in 2020 in Northeast China

297 (<https://www.resdc.cn>), (b) spatial distributions of the total number of fire spots during 2001-

298 2020 in Northeast China, and (c) seasonal distributions and errors of the annual fire spots from

299 2001 to 2020. The error is calculated as the number of fire spots identified by the traditional

300 method minus those extracted by the novel method.

301

302 Fire spots from open straw burning concentrated in spring and autumn, with few  
303 burning events in the other two seasons in Northeast China. Open straw burning events  
304 in this region during 2003-2020 can be roughly divided into three distinctive periods  
305 (**Fig. 2(c)**). During **Period I** (2003-2012), the annual average number of fire spots in  
306 this region was 3732. There were more fire spots in autumn than spring in most of  
307 these years. During **Period II** (2013-2017), there was a substantial surge in fire spots,  
308 with an annual average of 18,177 spots, accounting for 58.2% of the 20-year total.  
309 Notably, the number of fire spots peaked at 25,759 in 2014. Spring fire spots  
310 consistently increased annually, reaching the highest in 2017 at 12,094 spots. The  
311 variations for autumn fire spots were fluctuating, with a peak of 18,951 spots in 2014.  
312 During 2013-2015, autumn fire spots were higher than spring; however, this trend  
313 reversed in 2016 and 2017, with spring fire spots becoming more dominant. During  
314 **Period III** (2018-2020), the number of fire spots experienced a significant decrease,  
315 averaging 8,788 spots annually, which was a 51.7% decrease from **Period II**. Spring  
316 emerged as the primary season of fire spots, accounting for approximately 93.8% of the  
317 annual total. Zhao et al. (2021) have reported a similar phenomenon, in which the  
318 primary season of open straw burning in Northeast China gradually shifts to spring  
319 (April to June). The apparent seasonal variations of open straw burning primarily stems  
320 from strict government bans imposed after the autumn harvest (Yang et al., 2020). In  
321 addition, farmers' increasing awareness regarding how open straw burning contributes  
322 to the thawing of spring soil may also be a factor (Saxton et al., 1993; Song et al., 2024).

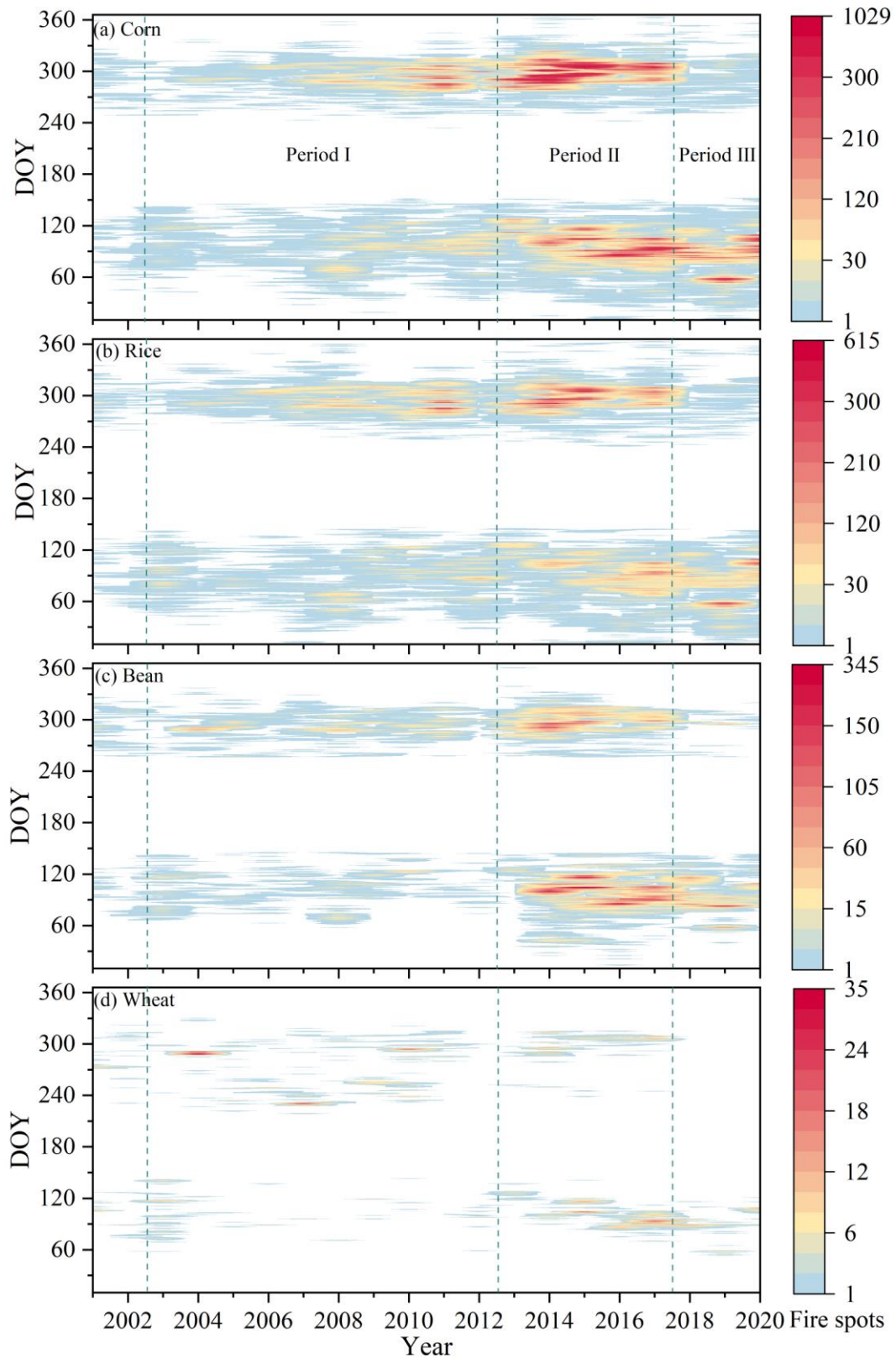
323

324 However, the “sudden drop” in fire spots should also be partially attributed to strategies  
325 employed by farmers to avoid detection by satellite and government regulations, such  
326 as burning straw on smaller scales and in more dispersed areas, or during non-transit  
327 times of the satellites (Liu et al. 2019; Liu et al. 2020). Chen et al. (2022) also found  
328 that farmers in East China frequently burned straw in 2019 during non-transit times of  
329 MODIS/VIIRS satellites, as indicated by Himawari satellite data. To further verify the  
330 reliability of the “sudden drop” in fire spots in Northeast China, we analyzed the trend  
331 of particulate matter concentrations ( $PM_{10}$  and  $PM_{2.5}$ ) during the periods of open straw  
332 burning from 2014 to 2020 in Northeast China (**Fig. S2**). Atmospheric particulate  
333 matter concentrations during autumn open straw burning in Northeast China decreased  
334 with a “sudden drop” in fire spots (**Fig. S2(c)**). However, a similar trend was not  
335 observed in spring (**Fig. S2(b)**), possibly due to limitations in fire spot detection by  
336 current satellite techniques and avoidance strategies. Kumar et al. (2021) suggested that  
337 a hybrid inventory, which accurately allocates emissions estimated using the “bottom-  
338 up” approach based on satellite data, may be more advantageous in this scenario.

339

340 The straw burning dates in Northeast China also changed during the three periods,  
341 besides varying with crop type. During **Period I** (2003-2012), the autumn burning dates  
342 of corn and rice straws were concentrated from **early October** to mid-November (DOY  
343 range of 270 to 320). Spring burning dates of corn and rice straw were concentrated

344 between mid-March and late April (DOY range of 70 to 120) in 2003, while dispersed  
345 to early March to mid-May (DOY range of 60 to 140) in 2012 (Fig. 3(a) and Fig. 3(b)).  
346 During Period II (2013-2017), the dispersion of spring burning dates for corn and rice  
347 straws became more pronounced, extending from early February to mid-May (DOY  
348 range of 30 to 140) (Fig. 3(a) and Fig. 3(b)). During Period III (2018-2020), the  
349 dispersion of spring burning dates for corn and rice straws persisted (Fig. 3(a) and Fig.  
350 3(b)). During Period I (2003-2012), the spring and autumn burning dates of bean straw  
351 in Heilongjiang Province were concentrated from mid-March to late April (DOY range  
352 of 70 to 120) and from early October to mid-November (DOY range of 270 to 320),  
353 respectively (Fig. 3(c)). During 2013-2020, the spring burning dates of bean straw in  
354 Northeast China were concentrated between early February and late April (DOY range  
355 of 30 to 120), while the autumn burning dates remained consistent with those during  
356 Period I in Heilongjiang Province (Fig. 3(c)). Unlike other crops, the burning dates for  
357 wheat straw did not conform to the aforementioned pattern of variation, likely due to a  
358 limited number of fire spots (Fig. 3(d)). The changing dispersion of burning dates for  
359 each crop type indicates shifts in agricultural practices that may be influenced by  
360 regional straw burning ban policies, environmental conditions, and farming practices  
361 (Yang et al., 2020).



362

363 **Fig. 3** The daily frequency distribution of fire spots from various straws burning: (a), (b), (c),

364 and (d) represent corn, rice, bean, and wheat straw, respectively. Note: The x-axis is Year; the

365 y-axis is DOY; and the daily number of fire spots for straw burning ranges from 1 to 1,029 for  
366 corn, 1 to 615 for rice, 1 to 345 for beans, and 1 to 35 for wheat.

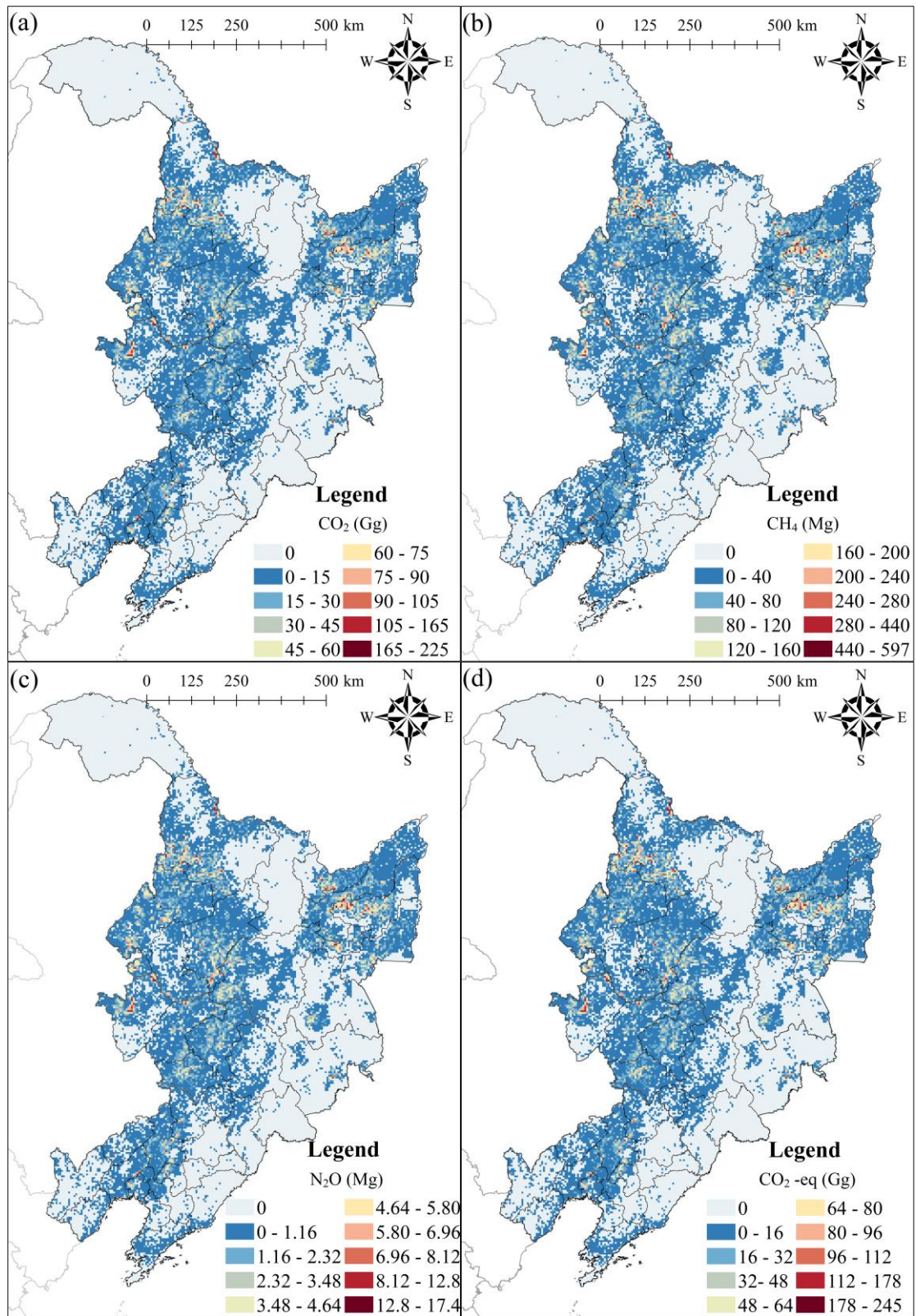
### 367 **3.2 High spatial resolution annual emission inventory of GHGs**

368 The cumulative emissions of CO<sub>2</sub>, CH<sub>4</sub>, and N<sub>2</sub>O from open straw burning in Northeast  
369 China from 2001 to 2020 amounted to 198 Tg, 557 Gg, and 15.7 Gg, respectively (or  
370 218 Tg CO<sub>2</sub>-eq in total). The spatial distributions of GHGs emissions correspond well  
371 with those of fire spots, particularly in high emission areas (**Fig. 2** and **Fig. 4**). However,  
372 the amounts of GHGs emissions in the northern Songnen Plain unexpectedly exceeded  
373 those in the eastern Songnen Plain and eastern Liao River Plain, suggesting that even  
374 low intensity fire spots can generate considerable emissions of GHGs due to higher  
375 FRP detected via remote sensing. Therefore, the FRP algorithm proves to be more  
376 effective than burned areas-based algorithms in identifying emission intensity resulted  
377 from open straw burning while reducing the uncertainty associated with high  
378 spatiotemporal resolution emission inventory (Wu et al., 2023).

379

380 The annual emissions of CO<sub>2</sub>, CH<sub>4</sub>, N<sub>2</sub>O, and CO<sub>2</sub>-eq from 2001 to 2020 are presented  
381 in **Figs. S3, S4, S5, and S6**, respectively. The spatiotemporal patterns of GHGs  
382 emissions correspond well to the observed trends in fire spots during **Period I (2003-**  
383 **2012)**. However, during **Period II (2013-2017)** and **Period III (2018-2020)**, the  
384 emissions of GHGs in the eastern Songnen Plain and eastern Liao River Plain did not  
385 exhibit a proportional increase with the rise in fire spots. This discrepancy can be

386 attributed to the dispersed burning dates among individual farmers in these regions,  
387 resulting in high intensity fire spots with relatively low emissions. In contrast, several  
388 State Farms located in the northern Sanjiang Plain and northern Songnen Plain  
389 demonstrated a higher level of synchronization in open straw burning activities,  
390 resulting in parallel trends between fire spots and emissions (Cui et al., 2021).



391

392 **Fig. 4** The cumulative GHGs emissions from open straw burning in Northeast China from 2001

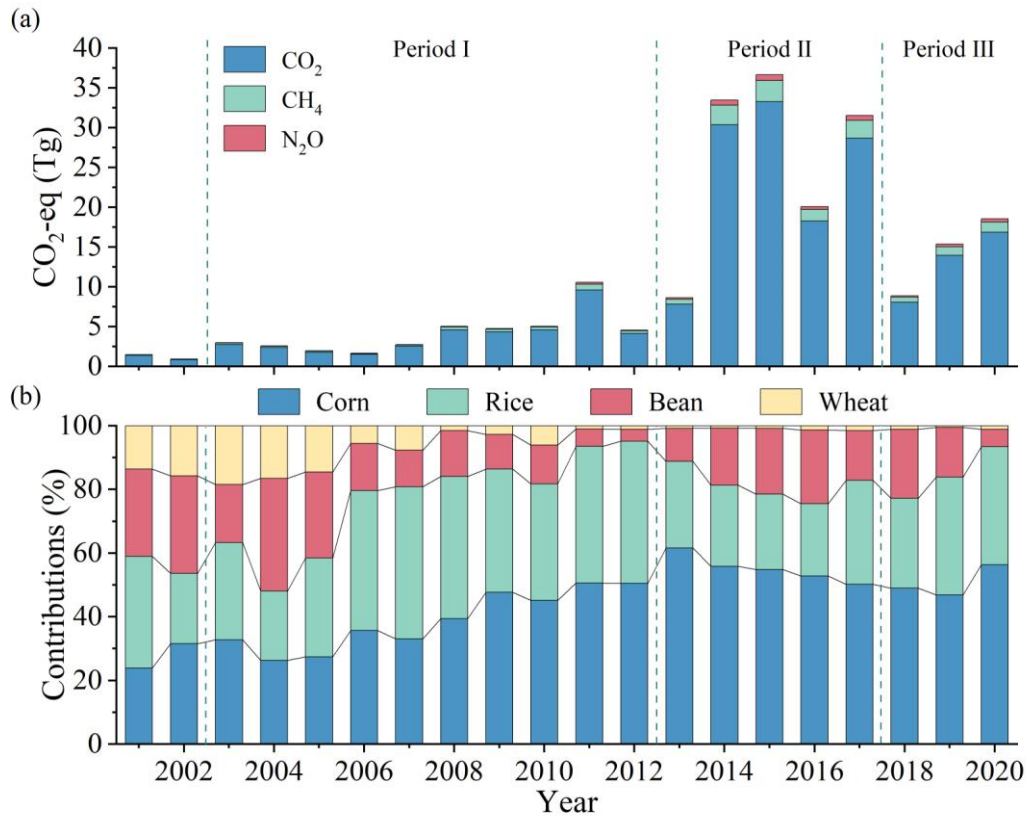
393 to 2020 for CO<sub>2</sub> (a), CH<sub>4</sub> (b), N<sub>2</sub>O (c), and CO<sub>2</sub>-eq (d) emissions, respectively.

394



395 During **Period I** (2003 - 2012), average annual CO<sub>2</sub>-eq emission was at 4.20 Tg, and  
396 the cumulative CO<sub>2</sub>-eq emission amounted to 42.0 Tg. During **Period II** (2013 - 2017),  
397 average annual CO<sub>2</sub>-eq emission increased substantially to 26.1 Tg, and the cumulative  
398 emission during this period amounted to 130 Tg, which accounted for 59.9% of the total  
399 emissions over the two decades. During **Period III** (2018 - 2020), average annual CO<sub>2</sub>-  
400 eq emissions decreased significantly to 14.3 Tg, and the cumulative emission during  
401 this period amounted to 42.8 Tg (**Fig. 5(a)**). The trend of CO<sub>2</sub>-eq emission from 2003  
402 to 2020 generally corresponds with the occurrence of fire spots, except for 2015 when  
403 higher emissions were obtained despite having fewer fire spots than the case in 2014  
404 (**Fig. 5(a)**). Such a trend is consistent with those of carbonaceous gases and aerosols  
405 (CGA) emissions estimated by Liu et al., (2022). This discrepancy between fire spots  
406 and pollutant emissions in 2015 highlights the limitations of estimating pollutant  
407 emissions based solely on burned areas (Ke et al., 2019; Wu et al. 2023). The  
408 combustion of corn and rice straw was identified as the primary contributors to CO<sub>2</sub>-eq  
409 emissions, accounting for 51.1% and 30.8%, respectively, of the total emissions (**Fig.**  
410 **5(b)**). Specifically, corn straw burning released 99.6, 9.06, and 2.42 Tg, while rice straw  
411 burning released 61.8, 3.78, and 1.27 Tg of CO<sub>2</sub>, CO<sub>2</sub>-eq for CH<sub>4</sub>, and CO<sub>2</sub>-eq for N<sub>2</sub>O,  
412 respectively.

413



414

415 **Fig. 5** (a) Regional total annual CO<sub>2</sub>-eq emissions and (b) percentage contributions from open

416 burning of individual crop straw type.

### 417 **3.3 Validation and limitations**

418 Our estimated total CO<sub>2</sub> emissions from 2012 to 2020 with MODIS (161 Tg) or with

419 VIIRS (165 Tg) were much lower than that (~ 523 Tg) estimated by Liu et al. (2022),

420 the latter was based on a modified FRP algorithm and fire spot products by VIIRS,

421 which has limitations in its traditional straw extraction methods in accurately

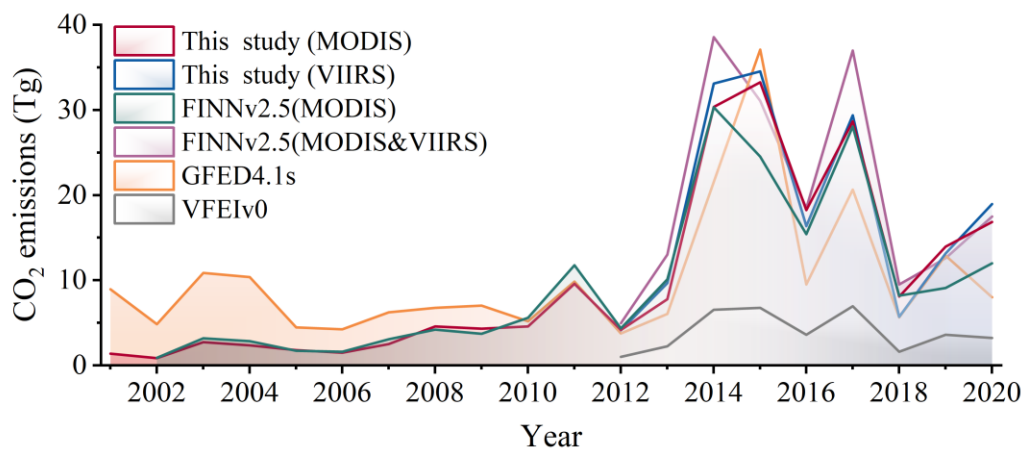
422 identifying fire spots during certain times of the year. Our estimated CO<sub>2</sub> emission from

423 2002 to 2020 in Northeast China (196 Tg) was slightly lower than that (195 Tg)

424 estimated by Global Fire Emissions Database Version 4.1 (GFED4.1s) by van der Werf et al.

425 (2017), and slightly higher than that (181 Tg) estimated from the Fire Inventory from

426 NCAR version 2.5 (FINNv2.5) by Wiedinmyer et al. (2023), which addresses the  
 427 underestimation of open biomass burning in China by the older version FINNv1.5  
 428 (Stavrakou et al., 2016; Yang et al., 2020) (Fig. 6). However, our estimated total CO<sub>2</sub>  
 429 emission from 2012 to 2020 was significantly higher than that (35.6 Tg) estimated by  
 430 VIIRS-based Fire Emission Inventory version 0 (VFEIv0) by Ferrada et al. (2022),  
 431 which relies on the traditional FRP algorithm (Fig. 6). Furthermore, Northeast China  
 432 surpassed East China (27.1 Tg) as the highest emitter from open straw burning in China  
 433 since 2014, with CO<sub>2</sub> emissions reaching 30.4 Tg (Zhang et al. 2020).



434  
 435 **Fig. 6** Annual total emissions of CO<sub>2</sub> from open straw burning (agricultural waste burning) in  
 436 Northeast China from this study with MODIS (red, 2001-2020) and VIIRS (blue, 2012-2020),  
 437 the Fire Inventory from NCAR version 2.5 (FINNv2.5) with MODIS-only (green, 2002-2020),  
 438 FINNv2.5 with MODIS and VIIRS (purple, 2012-2020), Global Fire Emissions Database  
 439 Version 4.1 (GFED4.1s) (orange, 2001-2020), and VIIRS-based Fire Emission Inventory  
 440 version 0 (VFEIv0) (grey, 2012-2020).

441

442 Although this study effectively improved the accuracy of emission inventory for open

443 straw burning through the novel method that integrates crop cycle information into  
444 extraction and classification of fire spots and the modified FRP algorithm, certain  
445 limitations still exist. The uncertainty in this study stems mainly from the inherent  
446 limitations of satellite fire detection systems. The MODIS fire spot product, although  
447 widely used, is limited by its temporal resolution and tends to miss transient or small-  
448 scale fires. In addition, straw burning during non-satellite transit periods, on cloudy  
449 days, at night, and under heavy haze further exacerbates the underestimation of fire  
450 incidence, leading to potential gaps in emission inventories.

451

452 Additionally, the novel method that integrates crop cycle information into extraction  
453 and classification of fire spots presents a promising advancement. However, its  
454 applicability is constrained to regions where comprehensive and detailed crop data are  
455 available. In countries or regions lacking such agricultural information, this method  
456 may face challenges, thereby limiting its broader applicability. These factors underscore  
457 the need for continued refinement of satellite detection technologies and the expansion  
458 of agricultural data collection efforts to reduce uncertainties and enhance the robustness  
459 of emission inventories on regional to global scales.

### 460 **3.4 Driving factors of open straw burning**

461 Open straw burning is more prominently influenced by anthropogenic activities  
462 compared to other types of open biomass burning, such as forest, shrubland, and  
463 grassland fires (Syphard et al., 2017; Wu et al., 2020). Open straw burning is influenced

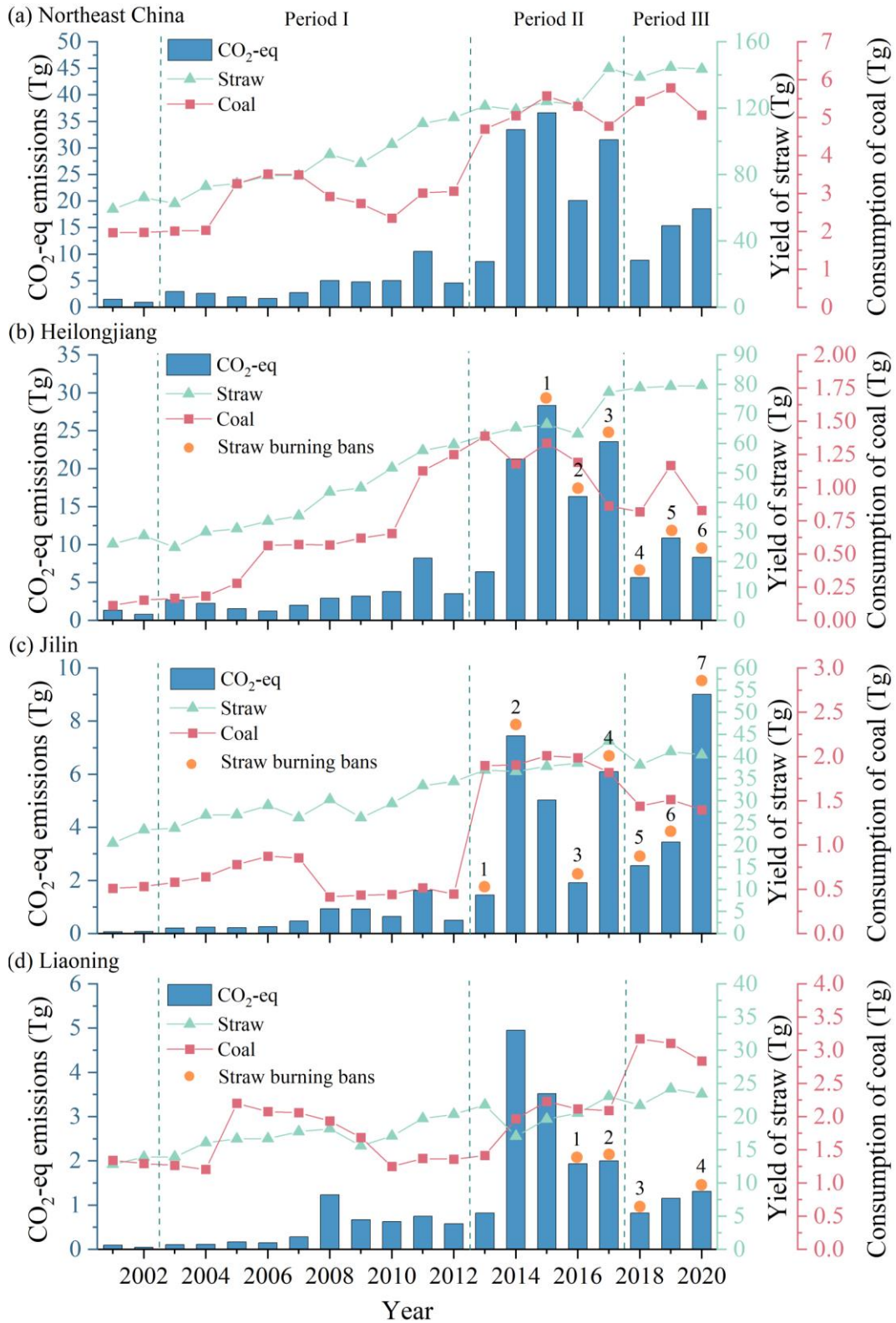
464 by changes in straw yield and utilization rate, straw burning ban policy, and farmers'  
465 awareness of straw burning consequences (Chen et al., 2016; Li et al., 2017; Tao et al.,  
466 2018; Fang et al., 2019; Xu et al., 2023b).

467

468 Northeast China has experienced a remarkable expansion in its sown area for major  
469 grain crops over the past two decades. By 2020, the sown area reached 231,937 km<sup>2</sup>,  
470 61.4% more than that in 2001 (National Bureau of Statistics of China, 2002-2021). In  
471 the meantime, annual straw yield reached 143 Tg in 2020, 142% higher than that (59.2  
472 Tg) in 2001 (**Fig. 7**) (numbers are calculated based on the major grain yields in  
473 Northeast China presented in National Bureau of Statistics of China (2002-2021) and  
474 the ratio of straw and grain (Wang et al., 2012)). Note that the annual straw yields have  
475 stabilized around 140 Tg since 2017, and this trend is expected to persist for many years  
476 to come (**Fig. 7**). From 2003 to 2020, a strong positive correlation was observed  
477 between the straw yields and the emissions of CO<sub>2</sub>-eq from open straw burning across  
478 Northeast China, as well as in Heilongjiang and Jilin provinces ( $p < 0.01$ , **Table S2**). If  
479 looking at individual periods, significant correlations were only observed during  
480 **Period I (2003-2012)** for the whole of Northeast China ( $p < 0.01$ ) and Heilongjiang ( $p$   
481  $< 0.01$ ) (**Table S2**). This highlights that increased straw yields exacerbated the  
482 challenges of straw disposal in Northeast China and have been a major contributor to  
483 the increase in the emissions of GHGs from open straw burning in the aforementioned  
484 region and period.

485

486 Besides open burning, crop straw is also used for cooking and heating in rural  
487 households in Northeast China (Ke et al., 2023; Liu et al., 2023). Crop straw can also  
488 be converted to bioenergy, used as animal feed, and returned to the fields (Alengebawy  
489 et al., 2022; Fang et al., 2022). However, exact quantification of straw utilization in  
490 different sectors in Northeast China is still lacking (Shi et al., 2023). Knowing that coal  
491 combustion and straw burning are major energy sources for rural households in  
492 Northeast China, we tried to explore potential changes in straw utilization on open straw  
493 burning through coal consumption changes (Fang et al. 2019). The abrupt increase in  
494 rural residential coal consumption in 2013 in Northeast China coincided with a spike in  
495 CO<sub>2</sub>-eq emissions from open straw burning (**Fig. 7(a)**). Furthermore, a significant  
496 positive correlation between rural residential coal consumption and CO<sub>2</sub>-eq emissions  
497 in Northeast China was revealed, especially in Heilongjiang and Jilin provinces (**Table**  
498 **S3**). We thus speculate that the increase in rural commercial energy consumption may  
499 have reduced the demand for straw as an energy source for agricultural households,  
500 thus facilitating the increased open straw burning. This needs to be confirmed in future  
501 studies once various straw utilization pathways are quantified.



502

503 **Fig. 7** Annual CO<sub>2</sub>-eq emissions, yield of straw, rural residential coal consumption, and straw

504 burning bans in (a) Northeast China, (b) Heilongjiang, (c) Jilin, and (d) Liaoning from 2001 to

505 2020.

506

507 We also evaluated the efficacy of straw burning ban policy in Heilongjiang, Jinlin, and  
508 Liaoning (**Table S4**). Despite the implementation of the policy since 2013 in this region,  
509 a significant reduction in CO<sub>2</sub>-eq emissions from open straw burning was only observed  
510 after 2018 (**Fig. 7**). Compared to the other regions of China, the effective control of  
511 open straw burning was delayed by several years in Northeast China (Huang et al.,  
512 2021). An important phenomenon was observed regarding the geographical and  
513 temporal expansion of the ban policy, e.g., initially focused on key areas and specific  
514 seasons (autumn and winter) and progressively extended to the entire region and  
515 throughout the whole year (see Heilongjiang Province as an example, **Table S4**).  
516 Therefore, enhanced enforcement of the ban policy likely reduced CO<sub>2</sub>-eq emissions  
517 during **Period III** and shifted the burning season to spring.

518

519 In conclusion, the enforcement of region-specific straw burning bans tailored to  
520 spatiotemporal variations is crucial to control GHGs emissions, given the anticipated  
521 sustained high straw yields in the future. Additionally, promoting diverse methods for  
522 utilizing straw is highlighted as an effective strategy for mitigating carbon emissions  
523 resulted from open straw burning in Northeast China. A combined effort on policy  
524 enforcement and alternative straw usage would play a pivotal role in addressing the  
525 environmental challenges posed by agricultural practices in the region.

526



## 527 4 Conclusions

528 This study provides a comprehensive analysis of the spatiotemporal variations of open  
529 straw burning across Northeast China from 2001 to 2020 and develops regional scale  
530 high spatial resolution annual emission inventories of GHGs. Open straw burning in  
531 Northeast China emitted a total of 218 Tg of CO<sub>2</sub>-eq during 2001-2020, of which 19.3%  
532 was from **Period I** (2003-2012), 59.9% from **Period II** (2013-2017), and 19.7% from  
533 **Period III** (2018-2020). Analysis results demonstrate the necessity of integrating the  
534 crop cycle information into the extraction and classification of fire spots from open  
535 straw burning to enhance the accuracy of emission inventories of various pollutants.  
536 This study also highlights the inconsistencies between the number of fire spots and  
537 pollutant emissions caused by remote sensing detection techniques. In Northeast China,  
538 regions such as the northern Sanjiang Plain, eastern and northern Songnen Plain, and  
539 eastern Liao River Plain are identified as high-emission areas of GHGs from open straw  
540 burning, which emitted 38.1, 45.5, 31.9, and 10.8 Tg of CO<sub>2</sub>-eq, respectively, during  
541 2001-2020. Additionally, it is observed that the season for open straw burning has  
542 shifted from autumn to spring, with dispersed burning dates. This spatiotemporal  
543 analysis provides crucial insights into policy effectiveness as well as geographical  
544 variations regarding compliance with regulations banning open straw burning.  
545 Consequently, government policies prohibiting open straw burning should be adjusted  
546 according to the observed spatiotemporal variations in different regions.  
547 Simultaneously promoting diversified applications of straw, such as bioenergy

548 conversion, animal feeding, and soil amendment, is recommended — a strategy that is  
549 aligned with China’s dual-carbon objectives aiming at achieving carbon peak and  
550 carbon neutrality.

551

## 552 **Conflict of interest**

553 The authors declare no conflict of interest.

## 554 **Acknowledgments**

555 This work was supported by the Distinguished Youth Science Foundation of  
556 Heilongjiang Province (JQ2023E001) and Young Leading Talents of Northeast  
557 Agricultural University (NEAU2023QNLJ-013).

558

## 559 **References**

560 Ahmed, W., Tan, Q., Ali, S., and Ahmad, N.: Addressing environmental implications of  
561 crop stubble burning in Pakistan: innovation platforms as an alternative approach, *Int.*  
562 *J. Global Warming*, 19, 76-93, <https://doi.org/10.1504/IJGW.2019.101773>, 2019.

563 Alengebawy, A., Mohamed, B.A., Ran, Y., Yang, Y., Pezzuolo, A., Samer, M., and Ai,  
564 P.: A comparative environmental life cycle assessment of rice straw-based bioenergy  
565 projects in China, *Environ. Res.*, 212, 113404,  
566 <https://doi.org/10.1016/j.envres.2022.113404>, 2022.

567 Chen, J.X., Li, R., Tao, M.H., Wang, L.L., Lin, C.Q., Wang, J., Wang, L.C., Wang, Y.,  
568 Chen, L.F.: Overview of the performance of satellite fire products in China:  
569 Uncertainties and challenges, *Atmos. Environ.*, 268, 118838,  
570 <https://doi.org/10.1016/j.atmosenv.2021.118838>, 2022.

571 Chen, Y.L., Shen, H.Z., Zhong, Q.R., Chen, H., Huang, T.B., Liu, J.F., Cheng, H.F.,  
572 Zeng, E.Y., Smith, K.R., and Tao, S.: Transition of household cookfuels in China from  
573 2010 to 2012, *Appl. Energ.*, 184, 800-809,  
574 <https://doi.org/10.1016/j.apenergy.2016.07.136>, 2016.

575 Cui, S., Song, Z.H., Zhang, L.M., Shen, Z.X., Hough, R., Zhang, Z.L., An, L.H., Fu,  
576 Q., Zhao, Y.C., and Jia, Z.Y.: Spatial and temporal variations of open straw burning  
577 based on fire spots in northeast China from 2013 to 2017, *Atmos. Environ.*, 244, 117962,  
578 <https://doi.org/10.1016/j.atmosenv.2020.117962>, 2021.

579 Fang, Y.R., Wu, Y., and Xie, G.H.: Crop residue utilizations and potential for bioethanol  
580 production in China, *Renew. Sust. Energ. Rev.*, 113, 109288,  
581 <https://doi.org/10.1016/j.rser.2019.109288>, 2019.

582 Fang, Y.R., Zhang, S.L., Zhou, Z.Q., Shi, W.J., and Xie, G.H.: Sustainable development  
583 in China: Valuation of bioenergy potential and CO<sub>2</sub> reduction from crop straw, *Appl.*  
584 *Energ.*, 322, 119439, <https://doi.org/10.1016/j.apenergy.2022.119439>, 2022.

585 Ferrada, G.A., Zhou, M., Wang, Jun., Lyapustin, A., Wang, Y.J., Freitas, S.R., and  
586 Carmichael, G.R.: Introducing the VIIRS-based Fire Emission Inventory version 0  
587 (VFEIv0), *Geosci. Model Dev.*, 15, 8085-8109, <https://doi.org/10.5194/gmd-15-8085->

588 2022, 2022.

589 Freeborn, P.H., Wooster, M.J., Hao, W.M., Ryan, C.A., Nordgren, B.L., Baker, S.P., and  
590 Ichoku, C.: Relationships between energy release, fuel mass loss, and trace gas and  
591 aerosol emissions during laboratory biomass fires, *J. Geophys. Res-Atmos.*, 113,  
592 D01301, <https://doi.org/10.1029/2007JD008679>, 2008.

593 Fu, J., Song, S.T., Guo, L., Chen, W.W., Wang, P., Duanmu, L.J., Shang, Y.J., Shi, B.W.,  
594 and He, L.Y.: Interprovincial joint prevention and control of open straw burning in  
595 Northeast China: Implications for atmospheric environment management, *Remote  
596 Sens.*, 14(11), 2528, <https://doi.org/10.3390/rs14112528>, 2022.

597 Gadde, B., Bonnet, S., Menke, C., and Garivait, S.: Air pollutant emissions from rice  
598 straw open field burning in India, Thailand and the Philippines, *Environ. Pollut.*, 157,  
599 1554-1558, <https://doi.org/10.1016/j.envpol.2009.01.004>, 2009.

600 Giglio, L., Schroeder, W., and Justice, C.O.: The collection 6 MODIS active fire  
601 detection algorithm and fire products, *Remote Sens. Environ.*, 178, 31-41,  
602 <https://doi.org/10.1016/j.rse.2016.02.054>, 2016.

603 Guan, Y.N., Chen, G.Y., Cheng, Z.J., Yan, B.B., and Hou, L.A.: Air pollutant emissions  
604 from straw open burning: A case study in Tianjin, *Atmos. Environ.*, 171, 155-164,  
605 <https://dx.doi.org/10.1016/j.atmosenv.2017.10.020>, 2017.

606 Hong, X., Zhang, C., Tian, Y., Wu, H., Zhu, Y., and Liu, C.: Quantification and  
607 evaluation of atmospheric emissions from crop residue burning constrained by satellite  
608 observations in China during 2016-2020, *Sci. Total. Environ.*, 865, 161237,

609 <https://doi.org/10.1016/j.scitotenv.2022.161237>, 2023.

610 [https://modis-fire.umd.edu/files/MODIS\\_C61\\_BA\\_User\\_Guide\\_1.1.pdf](https://modis-fire.umd.edu/files/MODIS_C61_BA_User_Guide_1.1.pdf)

611 [https://modis-fire.umd.edu/files/MODIS\\_C6\\_C6.1\\_Fire\\_User\\_Guide\\_1.0.pdf](https://modis-fire.umd.edu/files/MODIS_C6_C6.1_Fire_User_Guide_1.0.pdf)

612 Huang, K., Zhuang, G., Lin, Y., Wang, Q., Fu, J.S., Fu, Q., Liu, T., and Deng, C.: How  
613 to improve the air quality over megacities in China: pollution characterization and  
614 source analysis in Shanghai before, during, and after the 2010 World Expo, *Atmos.*  
615 *Chem. Phys.*, 13, 5927-5942, <https://doi.org/10.5194/acp-13-5927-2013>, 2013.

616 Huang, L., Zhu, Y.H., Liu, H.Q., Wang, Y.J., Allen, D.T., Ooi, M.C.G.,  
617 Manomaiphiboon, K., Latif, M.T., Chan, A., and Li, L.: Assessing the contribution of  
618 open crop straw burning to ground-level ozone and associated health impacts in China  
619 and the effectiveness of straw burning bans, *Environ. Int.*, 171, 107710,  
620 <https://doi.org/10.1016/j.envint.2022.107710>, 2023.

621 Huang, L., Zhu, Y.H., Wang, Q., Zhu, A.S., Liu, Z.Y., Wang, Y.J., Allen, D.T., and Li,  
622 L.: Assessment of the effects of straw burning bans in China: Emissions, air quality,  
623 and health impacts, *Sci. Total Environ.*, 789, 147935,  
624 <https://doi.org/10.1016/j.scitotenv.2021.147935>, 2021.

625 Huang, X., Li, M.M., Li, J.F., and Song, Y.: A high-resolution emission inventory of  
626 crop burning in fields in China based on MODIS Thermal Anomalies/Fire products,  
627 *Atmos. Environ.*, 50, 9-15, <https://doi.org/10.1016/j.atmosenv.2012.01.017>, 2012.

628 Jin, Q., Ma, X., Wang, W., Yang, S., and Guo, F.: Temporal and spatial variations of  
629 PM<sub>2.5</sub> emissions from crop straw burning in eastern China during 2000-2014. *Acta Sci.*

630 Circumstantiae, 37, 460-468, 2017. (in Chinese)

631 Jin, Q.F., Ma, X.Q., Wang, G.Y., Yang, X.J., and Guo, F.T.: Dynamics of major air  
632 pollutants from crop residue burning in mainland China, 2000-2014, J. Environ. Sci.,  
633 70, 190-205, <https://doi.org/10.1016/j.jes.2017.11.024>, 2018.

634 Ke, H.B., Gong, S.L., He, J.J., Zhou, C.H., Zhang, L., and Zhou, Y.K.: Spatial and  
635 temporal distribution of open bio-mass burning in China from 2013 to 2017, Atmos.  
636 Environ., 210, 156-165, <https://doi.org/10.1016/j.atmosenv.2019.04.039>, 2019.

637 Ke, Y.X., Zhang, F.X., Zhang, Z.L., Hough, R., Fu, Q., Li, Y.F., and Cui, S.: Effect of  
638 combined aging treatment on biochar adsorption and speciation distribution for Cd (II),  
639 Sci. Total Environ., 867, 161593, <http://doi.org/10.1016/j.scitotenv.2023.161593>, 2023.

640 Korontzi, S., McCarty, J., Loboda, T., Kumar, S., and Justice, C.: Global distribution of  
641 agricultural fires in croplands from 3 years of Moderate Resolution Imaging  
642 Spectroradiometer (MODIS) data, Global Biogeochem. Cy., 20, GB2021,  
643 <https://doi.org/10.1029/2005GB002529>, 2006.

644 Kumar, A., Hakkim, H., Sinha, B., and Sinha, V.: Gridded 1 km × 1 km emission  
645 inventory for paddy stubble burning emissions over north-west India constrained by  
646 measured emission factors of 77 VOCs and district-wise crop yield data, Sci. Total  
647 Environ., 789, 48064, [https://doi.org/10.1016/j.scitotenv.2021.](https://doi.org/10.1016/j.scitotenv.2021.148064)  
648 148064, 2021.

649 Li, C.L., Hu, Y.J., Zhang, F., Chen, J.M., Ma, Z., Ye, X.N., Yang, X., Wang, L., Tang,  
650 X.F., Zhang, R.H., Mu, M., Wang, G.H., Kan, H.D., Wang, X.M., and Mellouki, A.:

651 Multi-pollutant emissions from the burning of major agricultural residues in China and  
652 the related health-economic effects, *Atmos. Chem. Phys.*, 17, 4957-4988,  
653 <https://doi.org/10.5194/acp-17-4957-2017>, 2017.

654 Li, X.H., Wang, S.X., Duan, L., Hao, J.M., Li, C., Chen, Y.S., and Yang, L.: Particulate  
655 and trace gas emissions from open burning of wheat straw and corn stover in China,  
656 *Environ. Sci. Technol.*, 41(17), 6052-6058, <https://doi.org/10.1021/es0705137>, 2007.

657 Li, X.Y., Yu, L., Peng, D.L., and Gong, P.: A large-scale, long time-series (1984-2020)  
658 of soybean mapping with phenological features: Heilongjiang Province as a test case,  
659 *Int. J. Remote Sens.*, 42, 7332-7356, <https://doi.org/10.1080/01431161.2021.1957177>,  
660 2021.

661 Liu, L.H., Jiang, J.Y., and Zong, L.G.: Emission inventory of greenhouse gases from  
662 agricultural residues combustion: A case study of Jiangsu Province, *Environ. Sci.*, 32,  
663 1242-1248, 2011. (In Chinese)

664 Liu, T.J., Marlier, M.E., Karambelas, A., Jain, M., Singh, S., Singh, M.K., Gautam, R.,  
665 DeFries, R.S.: Missing emissions from post-monsoon agricultural fires in northwestern  
666 India: regional limitations of MODIS burned area and active fire products, *Environ.*  
667 *Res. Commun.*, 1, 011007, <https://doi.org/10.1088/2515-7620/ab056c>, 2019.

668 Liu, T.J., Mickley, L.J., Singh, S., Jain, M., DeFries, R.S., Marlier, M.E.: Crop residue  
669 burning practices across north India inferred from household survey data: Bridging  
670 gaps in satellite observations, *Atmos. Environ.* - X, 8, 100091,  
671 <https://doi.org/10.1016/j.aeaoa.2020.100091>, 2020.

672 Liu, Y.X., Zhao, H.M., Zhao, G.Y., Zhang, X.L., and Xiu, A.J.: Carbonaceous gas and  
673 aerosol emissions from biomass burning in China from 2012 to 2021, *J. Clean. Prod.*,  
674 362, 132199, <https://doi.org/10.1016/j.jclepro.2022.132199>, 2022.

675 Liu, Y.Z., Zhang, J., and Zhuang, M.H.: Bottom-up re-estimations of greenhouse gas  
676 and atmospheric pollutants derived from straw burning of three cereal crops production  
677 in China based on a national questionnaire, *Environ. Sci. Pollut. Res.*, 28, 65410-65415,  
678 <https://doi.org/10.1007/s11356-021-15658-9>, 2021.

679 Liu, Z.K., Cui, S., Fu, Q., Zhang, F.X., Zhang, Z.L., Hough, R., An, L.H., Li, Y.F., and  
680 Zhang, L.M.: Transport of neonicotinoid insecticides in a wetland ecosystem: has the  
681 cultivation of different crops become the major sources? *J. Environ. Manag.* 339,  
682 117838, <https://doi.org/10.1016/j.scitotenv.2023.161593>, 2023.

683 Luo, Y.C., Zhang, Z., Li, Z.Y., Chen, Y., Zhang, L.L., Cao, J., and Tao, F.L.: Identifying  
684 the spatiotemporal changes of annual harvesting areas for three staple crops in China  
685 by integrating multi-data sources. *Environ. Res. Lett.*, 15, 074003,  
686 <https://doi.org/10.1088/1748-9326/ab80f0>, 2020a.

687 Luo, Y.C., Zhang, Z., Chen, Y., Li, Z.Y., and Tao, F.L.: ChinaCropPhen1km: a high-  
688 resolution crop phenological dataset for three staple crops in China during 2000-2015  
689 based on leaf area index (LAI) products, *Earth Syst. Sci. Data*, 12, 197-214,  
690 <https://doi.org/10.5194/essd-12-197-2020>, 2020b.

691 Lv, Q.C., Yang, Z.Y., Chen, Z.Y., Li, M.C., Gao, B.B., Yang, J., Chen, X., and Xu, B.:  
692 Crop residue burning in China (2019-2021): Spatiotemporal patterns, environmental



693 impact, and emission dynamics, *Env. Sci. Ecotechnol.*, 21, 100394,  
694 <https://doi.org/10.1016/j.ese.2024.100394>, 2024.

695 Mehmood, K., Wu, Y.J., Wang, L.Q., Yu, S.C., Li, P.F., Chen, X., Li, Z., Zhang Y.B., Li,  
696 M.Y., Liu, W.P., Wang, Y.S., Liu, Z.R., Zhu, Y.N., Rosenfeld, D., and Seinfeld, J.H.:  
697 Relative effects of open biomass burning and open crop straw burning on haze  
698 formation over central and eastern China: modeling study driven by constrained  
699 emissions, *Atmos. Chem. Phys.*, 20, 2419-2443, [https://doi.org/10.5194/acp-20-2419-](https://doi.org/10.5194/acp-20-2419-2020)  
700 2020, 2020.

701 National Bureau of Statistics of China (NBSC): *China Statistical Yearbook*, China  
702 Statistics Press, Beijing, <http://www.stats.gov.cn/sj/ndsj/>, 2002-2021. (in Chinese)

703 Pan, X.L., Kanaya, Y., Taketani, F., Miyakawa, T., Inomata, S., Komazaki, Y., Tanimoto,  
704 H., Wang, Z., Uno, I., and Wang, Z.F.: Emission characteristics of refractory black  
705 carbon aerosols from fresh biomass burning: a perspective from laboratory experiments,  
706 *Atmos. Chem. Phys.*, 17, 13001-13016, <https://doi.org/10.5194/acp-17-13001-2017>,  
707 2017.

708 Peng, L.Q., Zhang, Q., and He, K.B.: Emissions inventory of atmospheric pollutants  
709 from open burning of crop residues in China based on a national questionnaire, *Res.*  
710 *Environ. Sci.*, 29, 1109-1118, 2016. (In Chinese)

711 Saxton, K.E., Kenny, J.F., and McCool, D.K.: Air permeability to define frozen soil  
712 infiltration with variable tillage and residue, *Trans. ASABE*, 36, 1369-1375,  
713 <https://dx.doi.org/10.13031/2013.28472>, 1993.

714 Schroeder, W., Oliva, P., Giglio, L., and Csiszar, I.A.: The New VIIRS 375 m active  
715 fire detection data product: Algorithm description and initial assessment, *Remote Sens.*  
716 *Environ.*, 143, 85-96, <https://dx.doi.org/10.1016/j.rse.2013.12.008>, 2014.

717 Shi, W.J., Fang, Y.R., Chang, Y.Y., and Xie, G.H.: Toward sustainable utilization of crop  
718 straw: Greenhouse gas emissions and their reduction potential from 1950 to 2021 in  
719 China, *Resour. Conserv. Recy.*, 190, 106824,  
720 <https://doi.org/10.1016/j.resconrec.2022.106824>, 2023.

721 Song, Z.H., Zhang, L.M., Tian, C.G., Li, K.Y., Chen, P.Y., Jia, Z.Y., Hu, P., and Cui,  
722 S.: Chemical characteristics, distribution patterns, and source apportionment of  
723 particulate elements and inorganic ions in snowpack in Harbin, China, *Chemosphere*,  
724 349, 140886, <https://doi.org/10.1016/j.chemosphere.2023.140886>, 2024.

725 Stavrakou, T., Müller, J.F., Bauwens, M., De Smedt, I., Lerot, C., Van Roozendael, M.,  
726 Coheur, P.F., Clerbaux, C., Boersma, K.F. van der A, R., and Song, Y.: Substantial  
727 underestimation of post-harvest burning emissions in the North China plain revealed  
728 by multi-species space observations, *Sci. Rep.*, 6, 32307,  
729 <https://dx.doi.org/10.1038/srep32307>, 2016.

730 Stockwell, C.E., Yokelson, R.J., Kreidenweis, S.M., Robinson, A.L., DeMott, P.J.,  
731 Sullivan, R.C., Reardon, J., Ryan, K.C., Griffith, D.W.T., and Stevens, L.: Trace gas  
732 emissions from combustion of peat, crop residue, domestic biofuels, grasses, and other  
733 fuels: configuration and Fourier transform infrared (FTIR) component of the fourth Fire  
734 Lab at Missoula Experiment (FLAME-4), *Atmos. Chem. Phys.*, 14, 9727-9754,

735 <https://doi.org/10.5194/acp-14-9727-2014>, 2014.

736 Sun, J.F., Peng, H.Y., Chen, J.M., Wang, X.M., Wei, M., Li, W.J., Yang, L.X., Zhang,  
737 Q.Z., Wang, W.X., and Mellouki, A.: An estimation of CO<sub>2</sub> emission via agricultural  
738 crop residue open field burning in China from 1996 to 2013, *J. Clean. Prod.*, 112, 2625-  
739 -2631, <https://dx.doi.org/10.1016/j.jclepro.2015.09.112>, 2016.

740 Syphard, A.D., Keeley, J.E., Pfaff, A.H., and Ferschweiler, K.: Human presence  
741 diminishes the importance of climate in driving fire activity across the United States, *P.*  
742 *Natl. Acad. Sci. U.S.A.*, 114, 13750-13755, <https://doi.org/10.1073/pnas.1713885114>,  
743 2017.

744 Tang, R., Huang, X., Zhou, D.R., and Ding, A.J.: Biomass-burning-induced surface  
745 darkening and its impact on regional meteorology in eastern China, *Atmos. Chem.*  
746 *Phys.*, 20, 6177-6191, <https://doi.org/10.5194/acp-20-6177-2020>, 2020.

747 Tao, S., Ru, M.Y., Du, W., Zhu, X., Zhong, Q.R., Li, B.G., Shen, G.F., Pan, X.L., Meng,  
748 W.J., Chen, Y.L., Shen, H.Z., Lin, N., Su, S., Zhuo, S.J., Huang, T.B., Xu, Y., Yun, X.,  
749 Liu, J. F., Wang, X.L., Liu, W.X., Cheng, H.F., and Zhu, D.Q.: Quantifying the rural  
750 residential energy transition in China from 1992 to 2012 through a representative  
751 national survey, *Nat. Energy*, 3, 567-573, <https://doi.org/10.1038/s41560-018-0158-4>,  
752 2018.

753 Tian, H., Zhao, D., and Wang, Y.: Emission inventories of atmospheric pollutants  
754 discharged from biomass burning in China, *Acta Sci. Circumstantiae*, 31, 349-357, 2011.  
755 (in Chinese)

756 Vadrevu, K., and Lasko, K.: Intercomparison of MODIS AQUA and VIIRS I-Band fires  
757 and emissions in an agricultural landscape-implications for air pollution research,  
758 Remote Sens., 10, 978, <https://doi.org/10.3390/rs10070978>, 2018.

759 van der Werf, G.R., Randerson, J.T., Giglio, L., van Leeuwen, T.T., Chen, Y., Rogers,  
760 B.M., Mu, M.Q., van Marle, M.J.E., Morton, D.C., Collatz, G.J., Yokelson, R.J., and  
761 Kasibhatla, P.S.: Global fire emissions estimates during 1997-2016, Earth Syst. Sci.  
762 Data, 9, 697-720, <https://doi.org/10.5194/essd-9-697-2017>, 2017.

763 Vermote, E., Ellicott, E., Dubovik, O., Lapyonok, T., Chin, M., Giglio, L., and Roberts,  
764 G.J.: An approach to estimate global biomass burning emissions of organic and black  
765 carbon from MODIS fire radiative power, J. Geophys. Res., 114, D18  
766 <https://doi.org/10.1029/2008jd011188>, 2009.

767 Wang, J.Y., Xi, F.M., Liu, Z., Bing, L.F., Alsaedi, A., Hayat, T., Ahmad., and Guan,  
768 D.D.: The spatiotemporal features of greenhouse gases emissions from biomass burning  
769 in China from 2000 to 2012, J. Clean. Prod., 181, 801-808,  
770 <https://doi.org/10.1016/j.jclepro.2018.01.206>, 2018.

771 Wang, X.Y., Xue, S., and Xie, G.H.: Value-taking for residue factor as a parameter to  
772 assess the field residue of field crops, J. China Agr. Univ., 17.1, 1-8, 2012. (in Chinese)

773 Weldemichael, Y., and Assefa, G.: Assessing the energy production and GHG  
774 (greenhouse gas) emissions mitigation potential of biomass resources for Alberta, J.  
775 Clean. Prod., 112, 4257-4264, <https://doi.org/10.1016/j.jclepro.2015.08.118>, 2016.

776 Wen, X., Chen, W.W., Chen, B., Yang, C.J., Tu, G., and Cheng, T.H.: Does the

777 prohibition on open burning of straw mitigate air pollution? An empirical study in Jilin  
778 Province of China in the post-harvest season, *J. Environ. Manage.*, 264, 110451,  
779 <https://doi.org/10.1016/j.jenvman.2020.110451>, 2020.

780 Wiedinmyer, C., Kimura, Y., McDonald-Buller, E.C., Emmons, L.K., Buchholz, R.R.,  
781 Tang, W.F., Seto, K., Joseph, M.B., Barsanti, K.C., Carlton, A.G., and Yokelson, R.:  
782 The Fire Inventory from NCAR version 2.5: an updated global fire emissions model for  
783 climate and chemistry applications, *Geosci. Model Dev.*, 16, 3873-3891,  
784 <https://doi.org/10.5194/gmd-16-3873-2023>, 2023.

785 Wiedinmyer, C., Yokelson, R.J., and Gullett, B.K.: Global emissions of trace gases,  
786 particulate matter, and hazardous air pollutants from open burning of domestic waste,  
787 *Environ. Sci. Technol.*, 48, 16, 9523-9530, <https://doi.org/10.1021/es502250z>, 2014.

788 Wooster, M.J., Roberts, G., Perry, G.L.W., and Kaufman, Y.J.: Retrieval of biomass  
789 combustion rates and totals from fire radiative power observations: FRP derivation and  
790 calibration relationships between biomass consumption and fire radiative energy  
791 release, *J. Geophys. Res-Atmos.*, 110, D24311, <https://doi.org/10.1029/2005JD006318>,  
792 2005.

793 Wu, B.B., Li, J.H., Yao, Z.L., Li, X., Wang, W.J., Wu, Z.C., and Zhou, Q.:  
794 Characteristics and reduction assessment of GHG emissions from crop residue open  
795 burning in China under the targets of carbon peak and carbon neutrality, *Sci. Total  
796 Environ.*, 905, 167235, <https://doi.org/10.1016/j.scitotenv.2023.167235>, 2023.

797 Wu, J., Kong, S.F., Wu, F.Q., Cheng, Y., Zheng, S.R., Qin, S., Liu, X., Yan, Q., Zheng,

798 H., Zheng, M.M., Yan, Y.Y., Liu, D.T., Ding, S., Zhao, D.L., Shen, G.F., Zhao, T.L., and  
799 Qi, S.H.: The moving of high emission for biomass burning in China: View from multi-  
800 year emission estimation and human-driven forces. *Environ. Int.*, 142, 105812,  
801 <https://doi.org/10.1016/j.envint.2020.105812>, 2020.

802 Wu, J., Kong, S.F., Wu, F.Q., Cheng, Y., Zheng, S.R., Yan, Q., Zheng, H., Yang, G.W.,  
803 Zheng, M.M., Liu, D.T., Zhao, D.L., and Qi, S.H.: Estimating the open biomass burning  
804 emissions in central and eastern China from 2003 to 2015 based on satellite observation,  
805 *Atmos. Chem. Phys.*, 18, 11623-11646, <https://doi.org/10.5194/acp-18-11623-2018>,  
806 2018.

807 Xu, R.B., Ye, T.T., Yue, X., Yang, Z.Y., Yu, W.H., Zhang, Y.W., Bell, M.L., Morawska,  
808 L., Yu, P., Zhang, Y.X., Wu, Y., Liu, Y.M., Johnston, F., Lei, Y.D., Abramson, M.J., Guo,  
809 Y.M., and Li, S.S.: Global population exposure to landscape fire air pollution from 2000  
810 to 2019, *Nature*, 621, 521-529, <https://doi.org/10.1038/s41586-023-06398-6>, 2023a.

811 Xu, C., and You, C.: Agricultural expansion dominates rapid increases in cropland fires  
812 in Asia, *Environ. Int.*, 179, <https://doi.org/108189>, 10.1016/j.envint.2023.108189,  
813 2023b.

814 Xu, W.D., Wooster, M.J., Kaneko, T., He, J.P., Zhang, T.R., and Fisher, D.: Major  
815 advances in geostationary fire radiative power (FRP) retrieval over Asia and Australia  
816 stemming from use of Himarawi-8 AHI, *Remote Sens. Environ.*, 193, 138-149,  
817 <https://dx.doi.org/10.1016/j.rse.2017.02.024>, 2017.

818 Xuan, F., Dong, Y., Li, J.Y., Li, X.C., Su, W., Huang, X.D., Huang, J.X., Xie, Z.X., Li,

819 Z.Q., Liu, H., Tao, W.C., Wen, Y.A., and Zhang, Y.: Mapping crop type in Northeast  
820 China during 2013-2021 using automatic sampling and tile-based image classification,  
821 Int. J. Appl. Earth Obs., 117, 103178, <https://doi.org/10.1016/j.jag.2022.103178>, 2023.

822 Yang, G.Y., Zhao, H.M., Tong, D.Q., Xiu, A.J., Zhang, X.L., and Gao, C.: Impacts of  
823 post-harvest open biomass burning and burning ban policy on severe haze in the  
824 Northeastern China, Sci. Total Environ., 716, 136517,  
825 <https://doi.org/10.1016/j.scitotenv.2020.136517>, 2020.

826 Yang, Y., and Zhao, Y.: Quantification and evaluation of atmospheric pollutant  
827 emissions from open biomass burning with multiple methods: a case study for the  
828 Yangtze River Delta region, China, Atmos. Chem. Phys., 19, 327-348,  
829 <https://doi.org/10.5194/acp-19-327-2019>, 2019.

830 Ying, L.X., Shen, Z.H., Yang, M.Z., and Piao, S.L.: Wildfire detection probability of  
831 modis fire products under the constraint of environmental factors: A study based on  
832 confirmed ground wildfire records, Remote Sens., 11, 24, 3031,  
833 <https://doi.org/10.3390/rs11243031>, 2019.

834 Zhang, X.H., Lu, Y., Wang, Q.G., and Qian, X.: A high-resolution inventory of air  
835 pollutant emissions from crop residue burning in China, Atmos. Environ., 213, 207-214,  
836 <https://doi.org/10.1016/j.atmosenv.2019.06.009>, 2019.

837 Zhang, T.R., de Jong, M.C., Wooster, M.J., Xu, W.D., and Wang, L.L.: Trends in eastern  
838 China agricultural fire emissions derived from a combination of geostationary  
839 (Himawari) and polar (VIIRS) orbiter fire radiative power products, Atmos. Chem.

840 [Phys., 20, 10687-10705, https://doi.org/10.5194/acp-20-10687-2020](https://doi.org/10.5194/acp-20-10687-2020), 2020.

841 Zhao, H.M., Yang, G.Y., Tong, D.Q., Zhang, X.L., Xiu, A.J., and Zhang, S.C.:

842 Interannual and seasonal variability of greenhouse gases and aerosol emissions from

843 biomass burning in Northeastern China constrained by satellite observations, *Remote*

844 *Sens.*, 13, 1005, <https://doi.org/10.3390/rs13051005>, 2021.

845 Zheng, B., Ciais, P., Chevallier, F., Yang, H., Canadell, J.G., Chen, Y., van der Velde,

846 I.R., Aben, I., Chuvieco, E., Davis, S.J., Deeter, M., Hong, C.P., Kong, Y.W., Li, H.Y.,

847 Li, H., Lin, X., He, K.B., and Zhang, Q.: Record-high CO<sub>2</sub> emissions from boreal fires

848 in 2021, *Science*, 379, 912-917, <https://doi.org/10.1126/science.ade0805>, 2023.

849 Zhou, Y., Xia, X.C., Lang, J.L., Zhao, B.B., Chen, D.S., Mao, S.S., Zhang, Y.Y., Liu, J.,

850 and Li, J.: A coupled framework for estimating pollutant emissions from open burning

851 of specific crop residue: A case study for wheat, *Sci. Total Environ.*, 844, 156731,

852 <https://doi.org/10.1016/j.scitotenv.2022.156731>, 2022.

853 Zhou, Y., Xing, X.F., Lang, J.L., Chen, D.S., Cheng, S.Y., Wei, L., Wei, X., and Liu, C.:

854 A comprehensive biomass burning emission inventory with high spatial and temporal

855 resolution in China, *Atmos. Chem. Phys.*, 17, 2839-2864, [https://doi.org/10.5194/acp-](https://doi.org/10.5194/acp-17-2839-2017)

856 [17-2839-2017](https://doi.org/10.5194/acp-17-2839-2017), 2017.

857 Zhuang, Y., Li, R.Y., Yang, H., Chen, D.L., Chen, Z.Y., Gao, B.B., and He, B.:

858 Understanding temporal and spatial distribution of crop residue burning in China from

859 2003 to 2017 using MODIS data, *Remote Sens.*, 10(3), 390,

860 <https://doi.org/10.3390/rs10030390>, 2018.



861 Zhu, C., Kawamura, K., and Kunwar, B.: Effect of biomass burning over the western  
862 North Pacific Rim: Wintertime maxima of anhydrosugars in ambient aerosols from  
863 Okinawa, *Atmos. Chem. Phys.*, 15, 1959-1973, [https://doi.org/10.5194/acp-15-1959-](https://doi.org/10.5194/acp-15-1959-2015)  
864 2015, 2015.